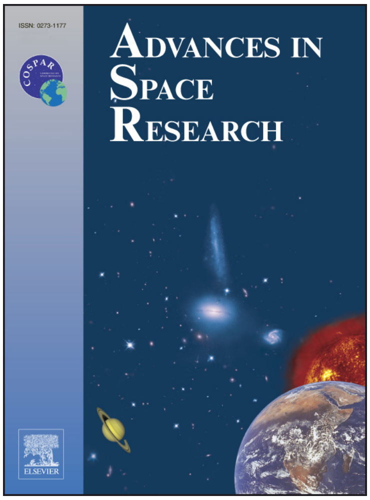

A new method to calculate the time delay of the Pi2 pulsations

Essam Ghamry, Adel Fathy

PII: S0273-1177(15)00764-4
DOI: http://dx.doi.org/10.1016/j.asr.2015.10.045
Reference: JASR 12500

To appear in: *Advances in Space Research*

Received Date: 24 April 2015
Revised Date: 26 October 2015
Accepted Date: 30 October 2015

Please cite this article as: Ghamry, E., Fathy, A., A new method to calculate the time delay of the Pi2 pulsations, *Advances in Space Research* (2015), doi: http://dx.doi.org/10.1016/j.asr.2015.10.045

Paper Title is:

A new method to calculate the time delay of the Pi2 pulsations

Authors are:

Essam Ghamry

National Research Institute of Astronomy and Geophysics, (NRIAG), 11421 Helwan, Cairo, Egypt.

Adel Fathy

Physics Department, Faculty of Science, Fayoum University, Egypt

Corresponding author is Essam Ghamry.

E-mail address: essamgh@yahoo.com and essamgh@nriag.sci.eg

Abstract

The time delay determination of the Pi2 pulsations could provide more understanding of the propagation characteristics of the Pi2. Few studies have concerned with the time delay of Pi2 pulsation. We present a new method to calculate the time delay of Pi2 pulsations using cross wavelet technique. We study 48 events occurred in March 2008 and February-May 2009 at Carson City (CCNV), McGrath (MCGR), The Pas (TPAS) and Kuujjuarapik (KUUJ) stations which belong to the ground magnetometer network of the Time History of Events and Macroscale Interactions during Substorms (THEMIS). The cross wavelet spectrum showed a comparable time with that obtained using cross correlation method. We suggest that the cross wavelet technique can be effectively used to calculate the time delay of Pi2 pulsation and further used as a substitute for cross correlation method.

Key words: Pi2 pulsation, time delay, cross wavelet.

Title: A new method to calculate the time delay of the Pi2 pulsations

Abstract

The time delay determination of the Pi2 pulsations could provide more understanding of the propagation characteristics of the Pi2. Few studies have concerned with the time delay of Pi2 pulsation. We present a new method to calculate the time delay of Pi2 pulsations using cross wavelet technique. We study 48 events occurred in March 2008 and February-May 2009 at Carson City (CCNV), McGrath (MCGR), The Pas (TPAS) and Kuujjuarapik (KUUJ) stations which belong to the ground magnetometer network of the Time History of Events and Macroscale Interactions during Substorms (THEMIS). The cross wavelet spectrum showed a comparable time with that obtained using cross correlation method. We suggest that the cross wavelet technique can be effectively used to calculate the time delay of Pi2 pulsation and further used as a substitute for cross correlation method.

Key word: Pi2 pulsation, time delay, cross wavelet.

Corresponding author is Essam Ghamry.

E-mail address: essamgh@yahoo.com and essamgh@nriag.sci.eg

The current affiliation:

National Research Institute of Astronomy and Geophysics, (NRIAG), 11421 Helwan, Cairo, Egypt.

Introduction

Geomagnetic Pi2 pulsations are irregular and damped ultra-low frequency wave naturally occurring in the Earth's magnetic field in the period range of 40s to 150s (Saito et al., 1969). They associate with the magnetic wave energy released during impulsive magnetic field dipolarization processes that characterized a substorm. As a result, substorm current wedge forms connecting magnetosphere and ionosphere (Clauer and McPherron, 1974; Lester et al., 1983). So, it can be a promising tool for determining the substorm onset. Pi2 pulsations can occur at all latitudes on the nightside with latitudinal and longitudinal variations in amplitude and phase (Yumoto, 1986). At high-latitude stations ($L > \sim5$), Pi2 can be observed in the auroral zone, beneath the substorm enhanced ionospheric electrojet (Olson et al. 1975). Pi2 at midlatitudes ($\sim2 \leq L \leq \sim5$) are appeared with a similar signature extending over at least 60° in longitude near the meridian of the substorm current wedge (Singer et al., 1983). At low latitudes ($L < \sim2$), Pi2s can be observed at almost all local times and are appeared even on the dayside (Sutcliffe and Yumoto, 1989). The generation mechanism of Pi2 varies with their characteristics, relation with in situ observation, and the location of Pi2 observation.There are several scenarios on the generation mechanisms of Pi2 pulsations such as surface wave at the plasmapause (Sutcliffe, 1975) excited by the incoming compressional waves from the tailward source; the plasmaspheric cavity modes (Allan et al., 1986; Zhu and Kivelson, 1989; Fujita and Glassmeier, 1995; Lee, 1996); plasmaspheric virtual resonance mode (Lee, 1998; Lee and Lysak, 1999; Takahashi, 2006; Ghamry et al., 2011; Ghamry et al., 2012; Ghamry et al., 2015). The Pi2 onset has many cautions due to different factors: [1] Pi2 amplitude has a gradual increase until it reaches its maximum (Yanagihara and Shimizu, 1966). [2] It has a propagation time from low latitude to high latitude region approximately 100 s in the H component; also it has a longitudinal propagation, so there is a time of flight between ground stations (Fan et al., 2000; Uozumi et al., 2004, 2007 and 2009). Nosé et al. (2012) on basis of their own method (Nose et al., 1998) have been proposed a new substorm index, the Wp index, which reflects Pi2 wave power at low-latitude using geomagnetic field data from 11 ground stations.

The time delay relation of Pi2 pulsation especially at high and low latitude region still an open question. There are a few studies that concerned with the time delay of Pi2 pulsation. Uozumi et al. (2000) showed the latitudinal propagation of Pi2 with respect to the relative timing of the maximum amplitude of Pi2 magnetic energy. Uozumi et al. (2004) used the same approach as Uozumi et al. (2000) to study the longitudinal and latitudinal Pi2 propagation in high-latitude region using the maximum time energy method of the wave packet $\Delta H^2 + \Delta D^2$. Uozumi et al. (2009) determined the propagation time of Pi2 pulsation between two ground stations. To do so, they combined the maximum time energy method and the cross correlation method. It has been difficult to determine the onset time of Pi2 pulsations with accuracy 15-30s or less due to the gradual increase of the magnetic perturbation around the onset. In the same time the higher latitudinal stations have ±1 minute identification of the substorm onset time of the magnetospheric substorm or substorm intensification (Rostoker et al., 1980). So it's too hard and inaccurate to determine the time of flight of the Pi2 pulsations in the time domain.

During the last decade, wavelet analysis proved to be a useful tool in space physics (Waters, 2000; Chaston et al., 2005; Hafez et al., 2012, 2013a and 2013b; Ghamry et al., 2013; Hafez and Ghamry, 2013). This work aims to use the cross wavelet technique as a new method to calculate the time delay of Pi2 pulsations between two stations separated by latitude. We make a comparison between the cross wavelet technique and the cross correlation method. We suggest that cross wavelet technique can be used as a substitute for cross correlation method. The outline of this paper is as follows. In section 2 we describe the data sets and event selection. In section 3 we present the applied methodology. In section 4 we show some advantages of cross wavelet technique through this study. In section 5 we present the results achieved by the analysis. In section 6 we give the conclusions.

2. Data Sets and event selection:

In this section, we describe the data used to calculate the propagation of Pi2 pulsations. Data obtained from Carson City (CCNV), Mcgrath (MCGR), The Pas (TPAS) and Kuujjuarapik (KUUJ) stations which belong to the ground magnetometer network of the Time History of Events and Macroscale Interactions during Substorms (THEMIS). The geomagnetic coordinates of these stations are listed in Table 1. The data from these stations have 0.5 second resolution.

Here is Table 1.

Pi2 pulsations were identified from the magnetic field horizontal component at all stations. We visually examined the Pi2 events occurred in the nighttime interval (1800 to 0600 local time) to exclude pulsations excited by solar wind disturbances. We identified 48 Pi2 events in March 2008 and February to May 2009. The CCNV station is the lowest latitudinal station in THEMIS network. We will compare CCNV with one of the higher latitudinal stations (MCGR, TPAS or KUUJ). Based on our criteria (in section 3), related to the correlation coefficient (>= 0.75), none of TPAS events match this condition while KUUJ is used only for 7 events. Figure 1 shows typical examples of the Pi2, where CCNV station in the left panels and the higher latitudinal station in the right panels.

Here is Figure 1.

3. Methodology

In this section we present cross correlation method and cross wavelet method and demonstrate their criteria for calculation the time delay.

3.1 Cross correlation (XC)

Through this method, the time delay was calculated using a built in MATLAB function xcorr. We use the following steps: first, the time series is filtered using high pass filter with cut off frequency 0.004 Hz. Second, 7-minutes length of the filtered data are selected starting from each Pi2 onset. We picked out 7-minutes data, 2-minutes before the maximum amplitude and 5-minutes after it, to cover at least two full cycles of Pi2 pulsation especially with large Pi2 period detected in our events. Finally, we calculated the time shift at the correlation coefficient >=0.75. Figure 2a shows high pass filtered data observed on February 17, 2009 at CCNV and MCGR stations. The selected 7 minutes for calculating the XC and the XC plot are shown in Figure 2b and Figure 2c, respectively. The maximum XC coefficient provided is 0.81. At this coefficient the time shift is equal +35s, the positive sign means the CCNV station leading the MCGR station by 35s.

Here is Figure 2.

3.2 Cross wavelet spectrum

3.2.1 A brief introduction about wavelet transformation

The wavelet transformation decomposes the time series signal $x(.)$ into its equivalent frequency-time pattern using a base wavelet function $\psi(.)$. The wavelet coefficients are calculated through a convolution of the signal with the basis functions in equation 2.

$$W_n(s) = \sqrt{\tfrac{dt}{s}} \sum_{n=1}^{N} x_n \psi_n^*[(n-n_0)\tfrac{dt}{s}] \tag{2}$$

Where dt, s, n and $\psi^*(.)$ are the sampling time interval, the scales, the shifting parameter and the complex conjugate of the base wavelet filter, respectively. This process could be performed faster in the Fourier space. The wavelet is a powerful analytical method for decomposing the time series because it contains wide types of filters which have different scales (frequency width) and shapes. We used the Morlet base wavelet function because it has a uniform distribution and limited in frequency. The length of the time series and the filter, both control the maximum number of levels Jth to which we can decompose the signal;

$$scale = \tfrac{N}{2} = s_0 * 2^J \tag{3}$$

Where N is the length of the time series and s_0 is the smallest scale which is twice the sampling time interval.

Here is Figure 3.

According to the same Pi2 event in Figure 2, Figures 3a and 3b show the raw data minus daily mean value (blue color) and filtered data (red color) at CCNV and MCGR, respectively. Figures 3c and 3d show the wavelet spectrum for CCNV and MCGR, respectively. It is clear that Pi2 at CCNV has a longer period than Pi2 at MCGR as indicated by the higher amplitude illustrated by the color coded index located in the right of each panel. The wavelet reveals an average period equals ~157s and ~132s at CCNV and MCGR, respectively.

3.2.2 Cross wavelet transformation (XWT)

The cross wavelet transformation (XWT) of two time series x_n *and* y_n is defined as $W^{XY}(s) = W^X(s)W^{Y*}(s)$ where W^{Y*} is the complex conjugate of the wavelet coefficients of the wavelet transform y_n. The absolute value of the complex XWT $|W^{XY}(s)|$, shows the time intervals and frequency ranges with high common power (Grinsted at al., 2004; Torrence and Compo, 1998).

The new work in this research is to use the XWT to detect time delay between two Pi2 events separated in latitude. The time difference between any pair of stations is calculated through:

$$\Delta t = \frac{T\,\Delta\phi}{2\pi} \tag{4}$$

Where T is the period of the maximum integrated power and $\Delta\phi$ is the circular phase shift in radian. The criteria in our study is as follows: we filter the raw data using high pass filter with cut off frequency 0.004 Hz. We calculate the integrated power at each frequency, then we determine the frequency at maximum integrated common power amplitude. We integrate the common power amplitude at each time step and select 7-minutes length within the maximum integrated power amplitude (2-minutes before maximum power amplitude and 5-minutes after it). Then, we determine the frequency at maximum power amplitude and we calculate the phase as a mean value of these 7-minutes. Finally we calculate the time delay according to equation 4. We also compare phase of the ±3 frequencies to illustrate how much time delay of these ±3 frequencies close to the dominant frequency. We found that the time delay of these ±3 frequencies have only ±5 seconds error. To show the phase angle and the power amplitude in one plot, we normalized power amplitude and multiplied by 150.

Figure 4a shows high pass filtered data at CCNV (blue color) and MCGR (red color) of the Pi2 event illustrated in Figure 2 and Figure 3. Figure 4b and 4c show the XWT and the phase angle with the normalized power amplitude, respectively. The relative phase relationship between the two stations is shown as arrows directions and phase values at locations that have correlation coefficients >=0.75. Left arrows direction means both stations are antiphase, while right arrows direction means both stations are in phase. The arrows in the downward direction means the lower latitudinal station (CCNV) leading higher latitudinal station (MCGR, KUUJ or TPAS) and vice versa. To avoid the confusion of the interpretation of the arrows direction, the X and Y notations refer to the lower and higher latitudinal stations, respectively. We can see, at the dominant period of the Pi 2 (157s), the direction of the arrows in the downward direction which means CCNV leading MCGR (X leading Y). The phase at this common integrated power is 71.2° and its corresponding time delay between CCNV and MCGR is equal to +33.5s, which is close to that calculated by the XC (+35s).

Here is Figure 4.

4. Advantages of cross wavelet technique

4.1 A Complex Pi 2 waveform with poor cross correlation coefficient

The XC sometimes mislead us to estimate the time delay, especially if the Pi2 event has a complicated waveform. Figure 5 shows a Pi2 pulsation observed on 1st May 2009. (a) CCNV (blue) and TPAS (red) high pass filtered data, (b, c, d, e) cross wavelet transformation and power amplitude, 07 minutes selected and cross correlation plot, respectively. The correlation coefficient is 0.72, which exclude the event from proceeding the time shift calculations (note that the time shift calculated at the correlation coefficient >=0.75). But the XWT showed that at a specific frequencies we have a high correlation coefficient >0.75. The time delay calculated by XC at 0.72 gives that X lead Y by 1.5s. While the XWT gives that X lead Y by 4.5s which close to XC value. So, we can conclude that the XWT can calculate the time delay with higher correlation coefficient.

Here is Figure 5.

4.2 Confused onset determination

Pi2 pulsations sometimes has no clear onset as observed on March 13, 2008 as shown in Figure 6, (a1, a2, b1, b2) show high pass filtered data in the upper panel and wavelet transformation in the lower panel for CCNV and MCGR, respectively; (c, d, e, f) show 7-minutes selected, cross correlation plot, cross wavelet transformation and power amplitude, respectively. The two solid rectangles show the selected event used to calculate the correlation coefficient for both stations. The data series (Figure 6b1) shows fluctuations observed at the beginning of the event (dashed rectangular). These fluctuations have higher frequency bands than that in the solid rectangular as seen at wavelet transformation (Figure 6b2). Thereby the calculations of the correlation coefficient will be affected by these higher frequencies. The XC of the selected time (Figure 6c and 6d) gave us two correlation coefficients (-0.8 and 0.79). Note that the amplitude of CCNV is multiplied by 3 to be visually clear. The highest correlation coefficient (-0.8) calculate the time delay that X leading Y by 39s while the lower correlation coefficient (0.78) gave Y leading X by 86s. In the same time, the XWT (Figure 6e) calculate a single time delay value equals -19s (Y leading X by 19s) at the dominant frequency (Figure 6f) regardless of the fluctuations in the time series. This indicates the capability of XWT method to calculate time delay more precisely than XC method.

Here is Figure 6.

5. Results

In this section we present the time delay results achieved by both XC and XWT methods. Table 2 shows a list of the 48 Pi2 pulsations: event number, date, start time, end time, time delay calculated by XC method, time delay calculated by XWT method, cross phase and the higher latitudinal station used with CCNV station.
Figures 7a and 7b show the relationship between the time delay and the Pi2 periods for XC and XWT, respectively. Note that the events in figure 7a are 96, reflecting the time delay based on XC, which occurred simultaneously at lower latitude station (CCNV) and one of higher latitude station. The events in figure 7b are 48 according to the unique definition of the period T associated with one event, determined by the maximum common power in the cross-wavelet spectrum (Eq. 4 and the subsequent explanation). Figure 7c shows a scatter plot of the time delay calculated by XC versus the time delay calculated by the XWT. A diagonal line, from (-60, -60) to (70, 70), shows that most of the points are clustered along this line. About 70 % of calculated time delay of the Pi2 pulsations had a good correlation between both XC and XWT methods (the correlation coefficient R = 0.69). The XC showed 6 events have negative time delay while the XWT showed 3 events. This results show that Pi2 has a time delay between the higher latitudinal stations and the lower one in the range of +70s. This result is similar to the previous studies reported by (Fan et al., 2000; Uozumi et al., 2009). We also found that about 32 % of the Pi2 pulsations had a period more than 150s which is the upper limit of Pi2 period, indicated by horizontal dashed line in Figures 7a and 7b, as defined by Jacobs et al. (1964). It is noted that deep minimum between solar cycles 23 and 24 was observed in 2008-2009 (e.g., Mrigakshi et al., 2013). Perhaps this factor has led to observe periods more than 150s for Pi2 pulsations as described by Troitskaya (1967) and recently confirmed by Kwon et al. (2013).

Here is Table 2.

Here is Figure 7.

6. Conclusion

We present a new method to calculate the time delay between two stations using cross wavelet transformation. It is clearly shown that we have a comparable time between cross correlation method and cross wavelet transformation method. The cross wavelet spectrum gives the exact time delay at the dominant Pi2 period. Also, it shows a flexibility to visually illustrate the lagged/delayed station and enables us to calculate the phase of each frequency in non-confusable way. We suggest that the cross wavelet technique can be effectively used to calculate the time delay of Pi2 pulsation and further used as a substitute for cross correlation method.

Acknowledgments

The authors gratefully acknowledge THEMIS for the use of data.

References

Allan, W., S. P. White, and E. M. Poulter, Impulse-excited hydromagnetic cavity and field-line resonances in the magnetosphere, Planet. Space Sci., 3d, 371, 1986.

Chaston, C. C., T. D. Phan, J. W. Bonnell, F. S. Mozer, M. Acuńa, M. L. Goldstein, A. Balogh, M. Andre, H. Reme, and A. Fazakerley, Drift-kinetic Alfve´n waves observed near a reconnection X-line in the Earth's magnetopause, Phys. Rev. Lett., 95, 065002, 2005.

Cheng, C. Christopher T. Russell, and Jih-Hong Shue. On the association of quiet-time Pi2 pulsations with IMF variations, Adv. Space Res, 43, 1118–1129, 2008.

Clauer, C. R., and R. L. McPherron, Mapping the local time– universal time development of magnetospheric substorms using mid- latitude magnetic observations, J. Geophys. Res., 79, 2811, 1974.

Fan Guo-Hua, Dan-Wen Wang, Tong-Qi Yao, and Ke-Li Han, Analysis on observational results of Pi2 geomagnetic pulsation in Henan region, Acta Seismologica Sinica, 13, 174-179, doi:10.1007/s11589-000-0007-x, 2000.

Fujita, S., and K. H. Glassmeier, Magnetospheric cavity resonance oscillations with energy flow across the magnetopause, J. Geomagn. Geoelectr., 47, 1277–1292, 1995.

Ghamry E, A. Mahrous, N. Yasin, A. Fathy and K. Yumoto, First Investigation of Geomagnetic Micropulsation, Pi 2, in Egypt, Sun and Geosphere, 6 (2), 2011.

Ghamry E, A. Mahrous, A. Fathy, N. Salama, K. Yumoto, Signatures of the low-latitude Pi 2 pulsations in Egypt. NRIAG Journal of Astronomy and Geophysics 1, 45–50, 2012.

Ghamry, E., A. G. Hafez, K. Yumoto, and H. Yayama, Effect of SC on frequency content of geomagnetic data using DWT application: SC automatic detection, Earth Planets Space, 2013.

Ghamry, E., K.-H. Kim, H.-J Kwon , D.-H Lee , J.-S Park , J. Choi , K. Hyun , W. Kurth , C. Kletzing and J. Wygant, Simultaneous Pi2 observations by the Van Allen Probes inside and outside the plasmasphere, J. Geophys. Res. Space Physics, 120, doi:10.1002/2015JA021095, 2015.

Grinsted. A., Moore J. C. and Jevrejeva. S., Application of the cross wavelet transform and wavelet coherence to geophysical time series, Nonlinear Processes in Geophysics, 11, 561–566, 2004.

Hafez, A. G., E. Ghamry, H. Yayama and K. Yumoto, A wavelet spectral analysis technique for automatic detection of geomagnetic sudden commencements, IEEE, Transaction of Geosciences and Remote Sensing, 50, 4503-4512, 2012.

Hafez, A. G. and E. Ghamry, Geomagnetic Sudden Commencement Automatic Detection via MODWT, IEEE, Transaction of Geosciences and Remote Sensing, 51, 1547-1554, 2013.

Hafez, A. G., E. Ghamry, H. Yayamab, K. Yumoto, Systematic examination of the geomagnetic storm sudden commencement using multi resolution analysis, Adv. Space Res., 51, 39–49, 2013a.

Hafez, A. G., E. Ghamry, H. Yayamab, K. Yumoto, Un-decimated discrete wavelet transform based algorithm for extraction of geomagnetic storm sudden commencement onset of high resolution records, Comp. & Geos., 51, 143–152, 2013b.

Jacobs, J. A., Y. Kato, S. Matsushita, and V. A. Troitskaya, Classification of geomagnetic micropulsations, J. Geophys. Res., 69, 180–181, 1964.

Kwon, H.-J., K.-H. Kim, C.-W. Jun, K. Takahashi, D.-H. Lee, E. Lee, H. Jin, J. Seon, Y.-D. Park, and J. Hwang, Low-latitude Pi2 pulsations during intervals of quiet geomagnetic conditions (Kp ≤ 1), J. Geophys. Res. Space Physics, 118, 6145-6153, doi:10.1002/jgra.50582, 2013.

Lee, D.-H., Dynamics of MHD wave propagation in the low-latitude magnetosphere, J. Geophys. Res., 101, 15,371, 1996.

Lee, D.-H., On the generation mechanism of Pi2 pulsations in the magnetosphere, Geophys. Res. Lett., 25, 583, 1998.

Lee, D.-H., and R. L. Lysak, MHD waves in a three-dimensional dipolar magnetic field: A search for Pi2 pulsations, J. Geophys. Res., 104, 28,691, 1999.

Lester, M., W. J. Hughes, and H. J. Singer, Polarization patterns of Pi2 magnetic pulsa- tions and the substorm current wedge, J. Geophys. Res., 88, 7958, 1983.

Mrigakshi, A. I., D. Matthiä, T. Berger, G. Reitz, R. F. Wimmer-Schweingruber, Estimation of Galactic Cosmic Ray exposure inside and outside the Earth's magnetosphere during the recent solar minimum between solar cycles 23 and 24, Adv. Space Res, 52, 979-987, 2013.

Murphy, K. R.., Ra, I. J., Mann 1, I. R., Walsh A. P., Milling, D.K and Kale A, The dependence of Pi2 waveforms on periodic velocity enhancements within bursty bulk flows, Ann. Geophys, 29, 493–509, 2011.

Nosé, M., T. Iyemori, L. Wang, A. Hitchman, J. Matzka, M. Feller, S. Egdorf, S. Gilder, N. Kumasaka, K. Koga, H. Matsumoto, H. Koshiishi, G. Cifuentes-Nava, J. J. Curto, A. Segarra, and C. Celik (2012), Wp index: A new substorm index derived from high-resolution geomagnetic field data at low latitude, Space Weather, 10, S08002, doi:10.1029/2012SW000785.

Nosé, M., T. Iyemori, M. Takeda, T. Kamei, D. K. Milling, D. Orr, H. J. Singer, E. W. Worthington, and N. Sumitomo (1998), Automated detection of Pi2 pulsations using wavelet analysis: 1. Method and an application for substorm monitoring, Earth Planets Space, 50, 773-783.

Olson, J. V., Rostoker G., Pi2 pulsations and the auroral electrojet. Planet Space Sci, 23, 1129–1139, 1975.

Rostoker, G., K, Kawasaki, S. I, Akasofu, J. Foster, R. A. GreenWald, Y. Kamide, A. T. Y Lui, R. L. Mcpherron, and C. T. Russel, Magnetosperic substorms-definition and signatures, J. Geophys. Res, 85, 1663. 1980.

Russell, C. T., P. J. Chi, D. J. Dearborn, Y. S. Ge, B. Kuo-Tiong, J. D. Means, D. R. Pierce, K. M. Rowe, and R. C. Snare, THEMIS ground-based magnetometers, Space Sci. Rev., 141, 389–412, 2008.

Saito, T, Geomagnetic pulsations, Space Sci. Rev., 10, 319–412, 1969.

Saito, T., K, Yumoto., Y. Koyama, Magnetic pulsations Pi 2 as a sensitive indicator of magnetic substorm, Planet. Space Sci., 24, 1029, 1976.

Singer, H. J., Hughes W J, Fougere P F, et al., The localization of Pi2 pulsations: Ground-satellite observations. J Geophys Res, 88, 7029–7036, 1983.

Sutcliffe, P. R., The association of harmonics in Pi2 power spectra with the plasmapause, Planet. Space Sci., 23, 1581–1587, 1975.

Sutcliffe, P. R., Yumoto K., Dayside Pi 2 pulsations at low latitudes. Geophys Res Lett, 16, 887–890, 1989.

Takahashi, K., R. E. Denton, R. R. Anderson, and W. J. Hughes. Mass density inferred from toroidal wave frequencies and its comparison to electron density, J. Geophys. Res., 111, A01201, doi:10.1029/2005JA011286, 2006.

Torrence, C. and Compo, G. P.: A practical guide to wavelet analysis, Bull. Am. Meteorol. Soc., 79, 61–78, 1998.

Troitskaya, V. A., Micropulsations and the state of the magnetosphere, in Solar-Terrestrial Physics, edited by J. W. King, and W. S. Newman, pp. 213–274, Academic Press, New York, 1967.

Uozumi, T., K. Yumoto, H. Kawano, A. Yoshikawa, J. V. Olson, S. I. Solovyev, and E. F. Vershinin, Characteristics of energy transfer of Pi 2 magnetic pulsations: Latitudinal dependence, Geophys. Res. Lett., 27, 1619, 2000.

Uozumi, T., et al., Propagation characteristics of Pi 2 magnetic pulsations observed at ground high-latitudes, J. Geophys. Res., 109, A08203, 2004.

Uozumi, T., H. Kawano, A. Yoshikawa, M. Itonaga, and K. Yumoto, Pi 2 source region in the magnetosphere deduced from CPMN data, Planet. Space Sci., 55, 849, 2007.

Uozumi, T., Kitamura, K., Abe, S., Tokunaga, T., Yoshikawa, A., Kawano, H., Marshall, R., Morris, R.J., Shevtsov, B.M., Solovyev, S.I., McNamara, D.J., Liou, K., Ohtani, S., Itonaga, M., Yumoto, K., Propagation characteristics of Pi 2 pulsations observed at high- and low-latitude MAGDAS/CPMN stations: a statistical study. J. Geophys. Res., 114, A11207, doi:10.1029/2009JA014163, 2009.

Waters, C. L., ULF resonance structure in the magnetosphere, Adv. Space Res., 25, 1541-1558, 2000.

Yanagihara, K., Shimizu, N., Equatorial enhancement of micropulsation Pi-2. Mem. Kakioka Magn. Obs. 12, 57–63, 1966.

Yumoto, K., Generation and propagation mechanisms of low latitude magnetic pulsations: A review. J Geophys., 60, 79–105, 1986.

Zhu, X., and M. G. Kivelson, Global mode ULF pulsations in a magnetosphere with a nonmonotonic Alfve´n velocity profile, J. Geophys. Res., 94, 1479, 1989.

Figure captions:

Figure 1. Examples of the Pi2 pulsations observed at lower latitudinal station (CCNV) in the left and the higher latitudinal stations for the same events in the right.

Figure 2. (a) filtered data of Pi2 event occurred on February 17, 2009 (b) 7 minutes selected plot (c) cross correlation plot

Figure 3. Wavelet transformation of the Pi2 event shown in Figure 2. (a) raw data (blue) and high pass filtered data (red) of CCNV, (b) raw data (blue) and high pass filtered data (red) of MCGR, (c and d) wavelet spectrum for CCNV and MCGR, respectively.

Figure 4. (a) CCNV (blue) and MCGR (red) high pass filtered data of Pi2 event shown in Figure 2 and 3, (b) cross wavelet transformation. The relative phase relationship is shown as arrows (with in-phase pointing right, antiphase pointing left). (c) power amplitude.

Figure 5. Pi2 event observed at CCNV and TPAS stations on 1st May 2009. (a) CCNV (blue) and TPAS (red) high pass filtered data, (b, c) cross wavelet transformation and power amplitude, respectively, (d, e) 7-minutes selected plot and cross correlation plot, respectively.

Figure 6. Illustration of a confusable Pi2 event observed on March 13, 2008. (a1, a2, b1, b2) high pass filtered data in the upper panel and wavelet transformation in the lower panel for CCNV and MCGR, respectively, (c, d, e, f) 7-minutes selected plot, cross correlation plot, cross wavelet transformation and power amplitude, respectively.

Figure 7. (a, b) the relationship between the time delay and the Pi2 periods for XC and XWT, respectively. The horizontal dashed lines show the maximum Pi2 period. (c) a scatter plot of the time delay calculated by XC versus the time delay calculated by the XWT. A diagonal line, from (-60, -60) to (70, 70), shows that most of the points are clustered along this line. The dashed line shows the linear fit between the time delay calculated by XC and XWT.

List of tables

Station	Code	Geog Lat.	Geog Long.	Mag Lat.	Mag Long.	L	Midnight (hh:mm)
Kuujjuaq	KUUJ	55.3	282.3	65.2	352.0	5.66	04:14
The Pas	TPAS	54.8	258.1	63.0	320.3	5.18	07:04
McGrath	MCGR	63.0	204.4	62.2	256.6	4.47	11:30
Carson City	CCNV	39.1	240.2	45.3	304.8	2.00	08:26

Table 1. The geographic and geomagnetic location of the stations (Russell et al., 2008).

No	Date yyyymmdd	Time (hh:mm) start - end	Time delay XC	Time delay XWT	Phase (degree)	High latitude station
1	20080313	07:20-07:45	31	-16.6	-50	MCGR
2	20080317	09:00-09:30	17.5	24	66.4	MCGR
3	20080317	10:20-10:40	14.5	15	70.3	MCGR
4	20090210	09:20-10:00	22	30	54.7	MCGR
5	20090217	07:15-07:35	35	33.5	71.2	MCGR
6	20090301	08:00-08:20	11	32.5	61	MCGR
7	20090301	08:19-08:35	-20	18.5	80	MCGR
8	20090315	08:15-08:30	-10	26	102.3	MCGR
9	20090315	08:40-09:00	29.5	26	76	MCGR
10	20090317	05:45-06:00	19.5	17	73.1	MCGR
11	20090319	08:15-08:45	20	23.8	57.7	MCGR
12	20090323	06:03-06:30	53	64.8	102	MCGR

13	20090331	07:50-08:20	21	19	37.7	MCGR
14	20090331	08:20-09:00	24	31	64	MCGR
15	20090404	07:50-08:20	29.5	40	74	MCGR
16	20090404	05:50-06:20	24	34	80.6	MCGR
17	20090405	07:40-07:55	-39	-40	-145	MCGR
18	20090407	11:50-12:10	-9	-8.6	-11	MCGR
19	20090408	06:10-06:30	12.5	16	42	MCGR
20	20090410	07:35-07:48	30	32	98	MCGR
21	20090410	07:50-08:05	23	21	56.2	MCGR
22	20090413	04:55-05:10	43	42	126	MCGR
23	20090413	07:45-07:58	28.5	33	91	KUUJ
24	20090413	07:58-08:10	26.5	19	85.9	KUUJ
25	20090414	09:04-09:16	17.5	19	75	MCGR
26	20090414	09:24-09:36	20.5	21	31.0	MCGR
27	20090419	06:45-07:00	11	21	42	MCGR
28	20090419	06:00-06:12	23.5	23	75.2	MCGR
29	20090420	05:25-05:45	49	45	140.5	KUUJ
30	20090422	06:25-06:40	4.5	7	14.6	KUUJ
31	20090422	07:30-07:45	32	27	68.5	MCGR
32	20090424	06:16-06:35	-15	31	75.1	MCGR
33	20090428	07:45-08:10	14	26	54.8	KUUJ
34	20090428	08:40-09:10	21	21	63.8	KUUJ
35	20090430	08:20-08:45	49	45	109	MCGR

36	20090504	04:00-04:30	18	17	44.9	MCGR
37	20090504	08:00-08:22	42	29	111.1	MCGR
38	20090504	08:20-08:37	38	40	100.2	MCGR
39	20090504	08:50-09:15	28	31	78.7	MCGR
40	20090505	04:48-05:12	9	6.9	10.5	MCGR
41	20090514	06:44-07:05	21	25	53.3	MCGR
42	20090514	07:25-07:45	19.5	27	71.1	MCGR
43	20090522	01:43-02:10	-2.5	4.6	10.2	KUUJ
44	20090523	06:40-07:00	11.5	7.4	44	MCGR
45	20090523	07:05-07:25	20	23	80.4	MCGR
46	20090525	08:30-09:00	20	22	66.5	MCGR
47	20090526	07:30-08:00	18.5	12.5	53.2	MCGR
48	20090531	09:15-09:45	10	6	29.7	MCGR

Table 2. List of forty eight Pi2 pulsations used in this study. Event number, date, start time, end time, time delay calculated by XC method, time delay calculated by XWT method, cross phase and the higher latitudinal station used with CCNV station.

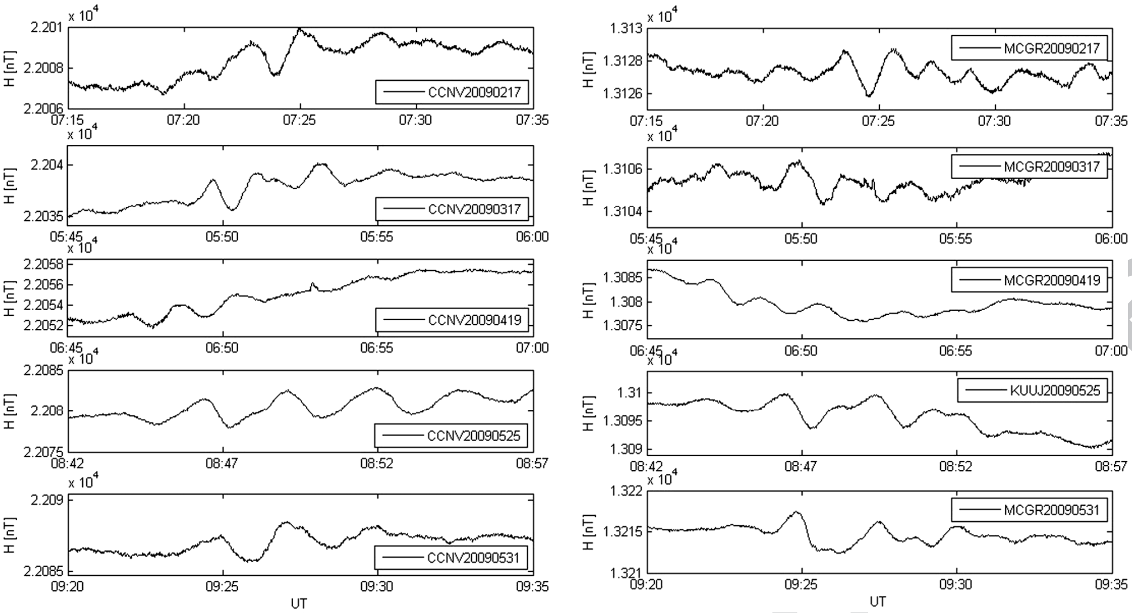
H [nT]
x 10^4
2.201
2.2008
2.2006
CCNV20090217
07:15
07:20
07:25
07:30
07:35
2.204
2.2035
CCNV20090317
05:45
05:50
05:55
06:00
2.2058
2.2056
2.2054
2.2052
CCNV20090419
06:45
06:50
06:55
07:00
2.2085
2.208
2.2075
CCNV20090525
08:42
08:47
08:52
08:57
2.209
2.2085
CCNV20090531
09:20
09:25
09:30
09:35
UT
1.313
1.3128
1.3126
MCGR20090217
1.3106
1.3104
MCGR20090317
1.3085
1.308
1.3075
MCGR20090419
1.31
1.3095
1.309
KUUJ20090525
1.322
1.3215
1.321
MCGR20090531

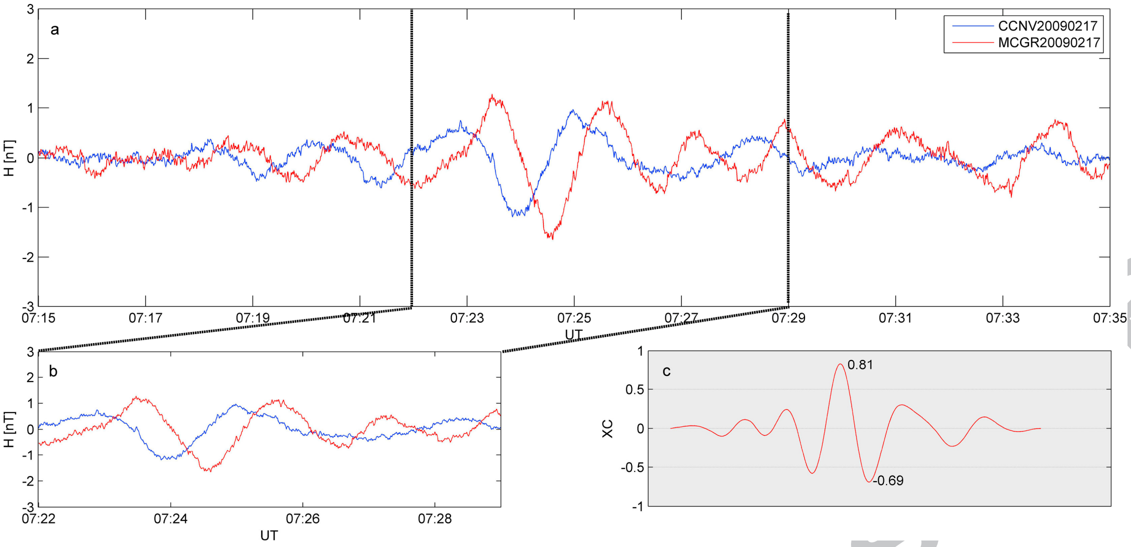
a
CCNV20090217
MCGR20090217
H [nT]
3
2
1
0
-1
-2
-3
07:15
07:17
07:19
07:21
07:23
07:25
07:27
07:29
07:31
07:33
07:35
UT
b
H [nT]
07:22
07:24
07:26
07:28
UT
c
XC
1
0.5
0
-0.5
-1
0.81
-0.69

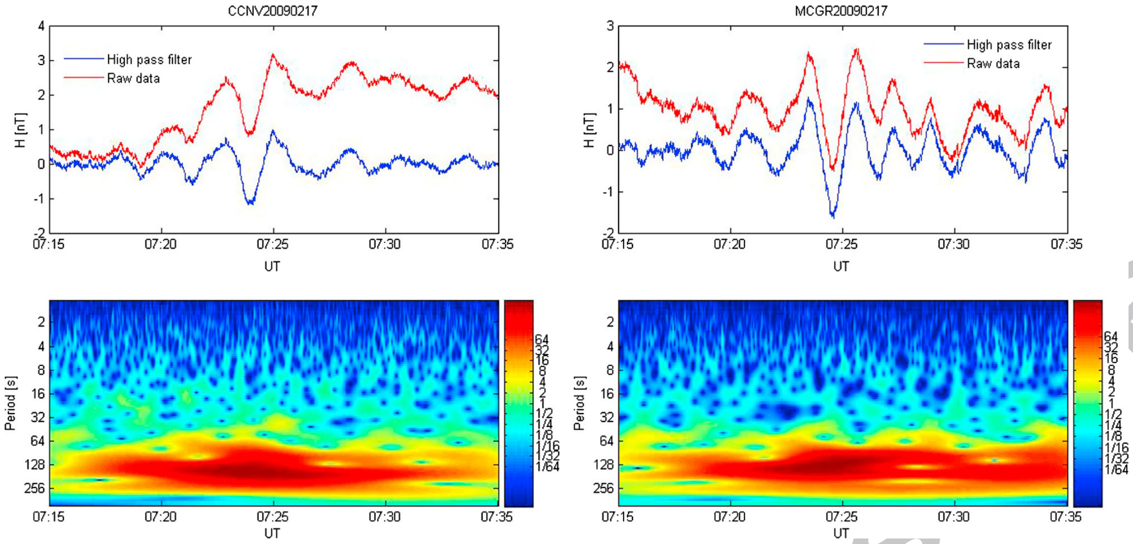
CCNV20090217
MCGR20090217
High pass filter
Raw data
H [nT]
UT
07:15
07:20
07:25
07:30
07:35
Period [s]
2
4
8
16
32
64
128
256
64
32
16
8
4
2
1
1/2
1/4
1/8
1/16
1/32
1/64

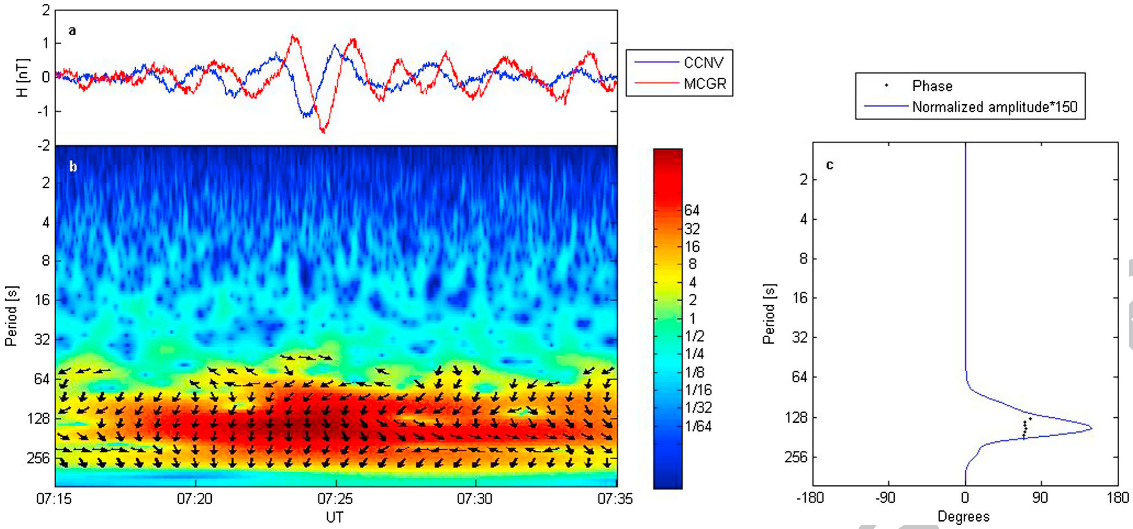
a
H [nT]
2
1
0
-1
-2
CCNV
MCGR
b
Period [s]
2
4
8
16
32
64
128
256
07:15
07:20
07:25
07:30
07:35
UT
64
32
16
8
4
2
1
1/2
1/4
1/8
1/16
1/32
1/64
Phase
Normalized amplitude*150
c
Period [s]
2
4
8
16
32
64
128
256
-180
-90
0
90
180
Degrees

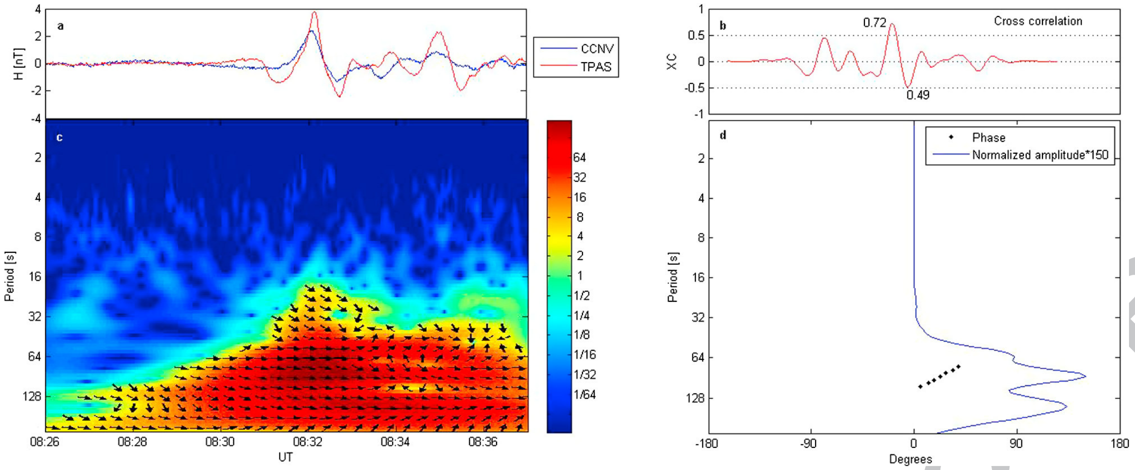
a
H [nT]
4
2
0
-2
-4
CCNV
TPAS
c
Period [s]
2
4
8
16
32
64
128
64
32
16
8
4
2
1
1/2
1/4
1/8
1/16
1/32
1/64
08:26
08:28
08:30
08:32
08:34
08:36
UT
b
XC
1
0.5
0
-0.5
-1
0.72
0.49
Cross correlation
d
Phase
Normalized amplitude*150
Period [s]
2
4
8
16
32
64
128
-180
-90
0
90
180
Degrees

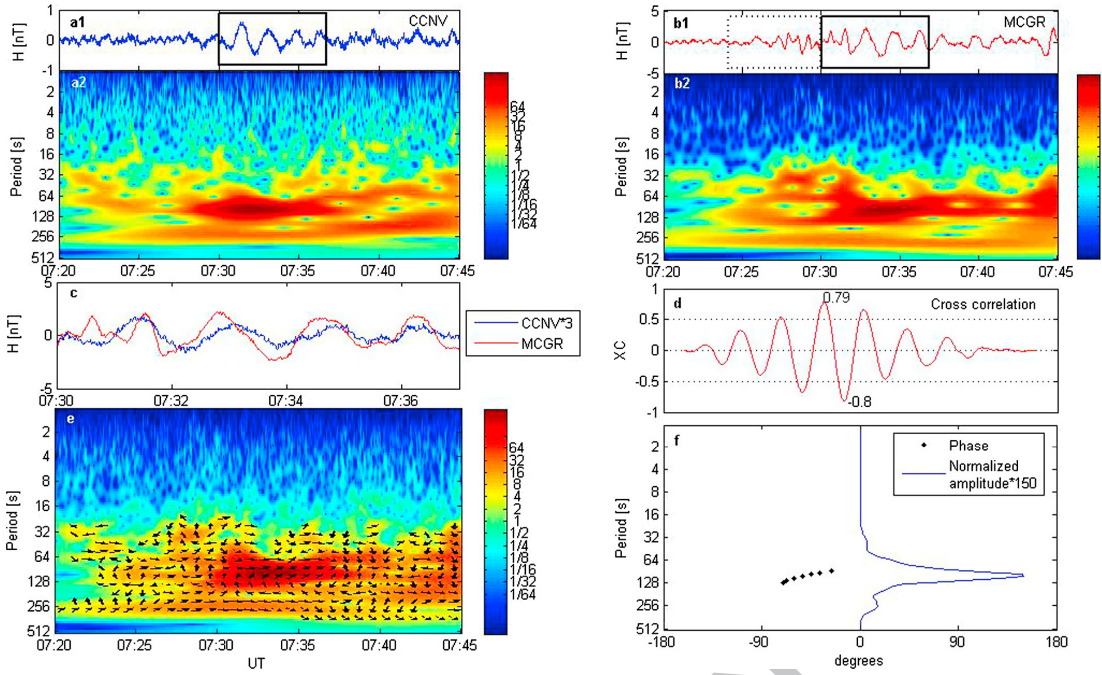
a1
CCNV
H [nT]
1
0
-1
a2
Period [s]
2
4
8
16
32
64
128
256
512
07:20
07:25
07:30
07:35
07:40
07:45
64
32
16
8
4
2
1
1/2
1/4
1/8
1/16
1/32
1/64
b1
MCGR
5
0
-5
b2
c
CCNV*3
MCGR
07:30
07:32
07:34
07:36
d
Cross correlation
XC
0.79
-0.8
0.5
-0.5
e
UT
f
Phase
Normalized amplitude*150
-180
-90
0
90
180
degrees

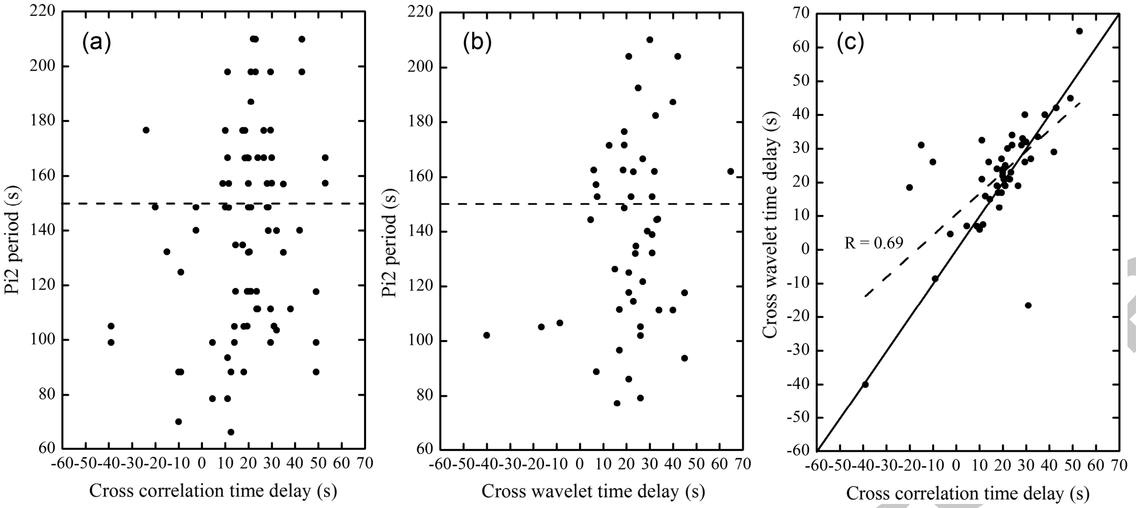
(a)
Pi2 period (s)
Cross correlation time delay (s)
(b)
Pi2 period (s)
Cross wavelet time delay (s)
(c)
Cross wavelet time delay (s)
Cross correlation time delay (s)
R = 0.69